High Buckling Strength of Auxetic Carbon Fiber Composite Laminates

ANTHONY TRICARICO, WENHUA LIN and YEQING WANG

ABSTRACT

This research focused on testing the effect of the negative Poisson's ratio of a carbon fiber composite on its critical buckling load. A secondary goal was to determine the accuracy of simulation compared to the experimental results for carbon fiber composites. In order to accomplish these two goals, both simulation and experimental testing were employed. For the simulation, ABAQUS software was used to determine predicted values for the critical buckling loads of auxetic and non-auxetic composites as well as the respective nonlinear force behavior of these composites. These results were then compared to experimental results of four auxetic and four non-auxetic specimens each experiencing uniaxial compressive tests. The results of simulation and experimentation showed that the critical buckling loads, and force sustained in general, of the auxetic composites were about three times higher than those of non-auxetic composites. While it appears that the negative Poisson's ratio has a significant impact on the buckling strength of composite materials, further testing is required to determine the effects of other factors on the critical buckling loads. Along with this, the simulation was more accurate for the auxetic composites than for the non-auxetic composites. Therefore, further testing and simulation are required to determine the limits of simulation accuracy for composite structures.

Anthony Tricarico, Master student, Department of Mechanical & Aerospace Engineering, Syracuse University, Syracuse, NY 13244
Wenhua Lin, PhD student, Department of Mechanical & Aerospace Engineering, Syracuse University, Syracuse, NY 13244
Yeqing Wang (corresponding author, email: ywang261@syr.edu), Assistant Professor, Department of Mechanical & Aerospace Engineering, Syracuse University, Syracuse, NY 13244

INTRODUCTION

Carbon fiber composites have been increasingly used in recent decades to build structures due to their light weight, high specific strength, and high specific stiffness compared to conventional materials such as metals [1-3]. These characteristics are an important consideration for uses in aerospace, wind energy, civil infrastructure, marine, and high-end sport structures [2-10]. In these applications, the strength of the composites must be comparable to metals to justify the substitution. Therefore, a goal for the future of composites is to continue to increase their strength without compromising their weight-saving benefits. The strength of fiber reinforced composite materials can be tested by different failure methods [11-16]. One type of failure that has been rarely tested for composites is the Euler buckling strength of which Euler buckling occurs when the compressive load on a structure causes out of plane deformation.

Poisson's ratio is a material characteristic that affects the Euler buckling behavior of composites. It is the negative ratio of the change in transverse strain to the change in axial strain. Most materials are non-auxetic which means that they have a positive Poisson's ratio [17]. Theoretically, this means that as the material is compressed transversely, it expands axially and vice versa [17]. On the other hand, there are fewer natural materials which possess a negative Poisson's ratio. They are called auxetic materials. Theoretically, this means that their axial and transverse strain have a direct relationship, they either both increase or both decrease [17]. This unique behavior may suggest that the material could locally flow into the buckling site to enhance the buckling strength. Therefore, it is expected that the buckling strength of composites can be increased by designing composites using an auxetic layup vs. an equivalent traditional non-auxetic layup. This means that changing a carbon fiber composite from non-auxetic to auxetic should theoretically increase its critical buckling load while having no significant impact on the weight. In this study, auxetic laminates were manufactured by using specific layup sequences identified, the non-auxetic counterparts were designed with layups that would allow them to produce identical effective modulus in the three principal directions with that of the auxetic specimens. This will isolate the coupling effect between the stiffness and the negative Poisson's ratio [18-21].

Another advancement in engineering is the use of simulation software in the design process. Whereas in the past, the design process consisted of designing, manufacturing, testing, and editing, now, simulation eliminates the need for manufacturing and experimental testing which results in a faster and more efficient design process [22]. For carbon fiber composites in particular, this speeds up the process by eliminating the fabrication periods before testing that require long time periods. As a result, simulation in the field of composite structures can play an important role in creating a more efficient design process.

EXPERIMENTAL SETUP

Materials and Specimens:

Similar to our previous study [23], the CFRP composite specimens used in this study were manufactured with unidirectional IM7/977-3 carbon fiber prepregs by

Table I. Comparison of predicted and measured Poisson's ratio and Young's modulus of auxetic and non-auxetic laminates.

	Auxetic Laminate [15/65/15/65/15]	**Non-auxetic Laminate [35/60/-5/60/35]**
Predicted Poisson's ratio	-0.41	0.16
Measured Poisson's ratio	-0.41 ± 0.012	0.16 ± 0.005
Predicted Young's modulus (GPa)	51.29	51.29
Measured Young's modulus (GPa)	52.14 ± 0.896	52.12 ± 0.774

following the recommended cure cycle. Using a layup orientation of [15/65/15/65/15] for the auxetic specimens and [35/60/-5/60/35] for the non-auxetic specimens, two 304.8 mm by 304.8 mm auxetic and non-auxetic CFRP plates were fabricated, respectively. After curing, four specimens with dimensions of 30 mm wide by 139.7 mm long, and a final thickness of 0.7 mm, were cut from the respective auxetic and non-auxetic laminates for the uniaxial compressive tests.

Table I shows the comparison between the predicted and measured Poisson's ratio and Young's modulus of auxetic and non-auxetic laminates. In the current study, the predicted in-plane Poisson's ratio for the auxetic laminate with a layup of [15/65/15/65/15] is -0.41, and for the non-auxetic laminate with a layup of [35/60/-5/60/35] is 0.16. As can be seen, the predicted and measured Poisson's ratio and Young's modulus are in good agreement with each other. Note that the layup of the non-auxetic laminate is specifically chosen to produce the same Young's modulus with the auxetic laminate. By doing so will allow us to investigate only the effect of Poisson's ratio on the critical buckling loads of composite laminates by avoiding differences in the respective Young's modulus.

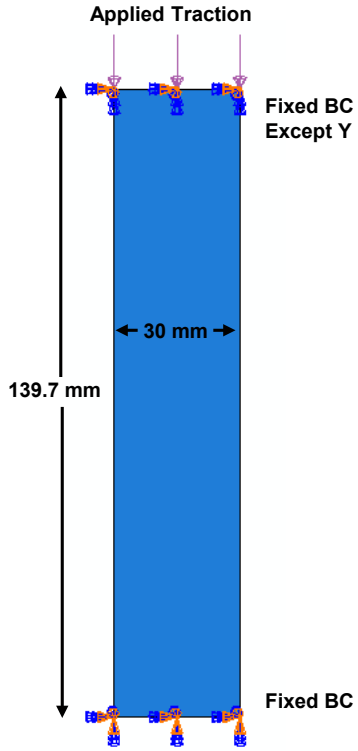

Figure 1. Schematic of the composite specimen using shell model in ABAQUS [15/65/15/65/15] for the auxetic model and [35/60/-5/60/35] for the non-auxetic model.

Simulation Setup:

The research in this discipline consisted of two separate procedures to compare the critical buckling loads of auxetic and non-auxetic carbon fiber composites. For the simulation, the finite element analysis software ABAQUS was employed. Prior to running the simulation, models were developed in the ABAQUS software for the auxetic and non-auxetic composite beams that were made for the experimental tests, as shown in Fig. 1. The model started out as a rectangular shell model with the same length and width as the testing specimens, *i.e.,* 139.7 mm by 30 mm. Next, the elastic material properties of the IM7/977-3 unidirectional prepreg were assigned. Finally, using that material, a conventional shell composite layup was employed with 5 layers of the composite material each with a thickness of 0.14 mm and with layups of [15/65/15/65/15] for the auxetic model and [35/60/-5/60/35] for the non-auxetic model.

The first procedure is a simulation of the computational model to determine the theoretical results. First, a step is added for a linear perturbation procedure type of "Buckle". For this step, the number of eigenvalues requested was 5, the vectors used per iteration is 10, and the maximum number of iterations was 300. Next, the boundary conditions were applied as depicted in Fig. 1. At the bottom edge, a fixed boundary condition is applied with no linear movement or rotation in any direction. At the top edge, the model was allowed to move in the y-direction, but movement was fixed in all other linear directions and in all rotational directions. Lastly, at the top edge, a compressive shell edge load was applied with a uniform distribution and a magnitude of 1. After this, a uniform mesh was applied to the model with a global size of 2 mm^2. Finally, a job was created to compile the results. Note that up to this point, the model only represented the results for linear buckling.

For nonlinear buckling behavior, the created model was modified by editing the keywords in the input file to include the imperfections in the subsequent nonlinear model. Next, the simulation step was changed to a general procedure type of "Static, Riks". For incrementation, the maximum number of increments was 100, the arc length increment had an initial value of 0.01, a minimum of 1e-5, and a maximum of 1e36, and the estimated total arc length was 1. Due to the change of simulation step, the boundary conditions and loads needed to be reapplied to the second model, with the only change being that the magnitude of the load is now equal to the value of the eigenvalue from the linear buckling results. After this, a second job was created for the nonlinear buckling model. Following this, the keywords for the second model were also modified to include an imperfection for the nonlinear model. Now the job can be run for nonlinear results. This process was done for both the auxetic and non-auxetic composite structures.

Uniaxial Compressive Test Setup:

The setup for the experimental test required a universal testing machine to apply the load and a fixture to be attached to the testing machine to impose the boundary conditions. Fig. 2 shows the uniaxial compressive test setup. The in-house fixture consists of two steel rectangular base pieces each with two sliders on one face that can be adjusted by tightening or loosening the two bolts inserted through each slider

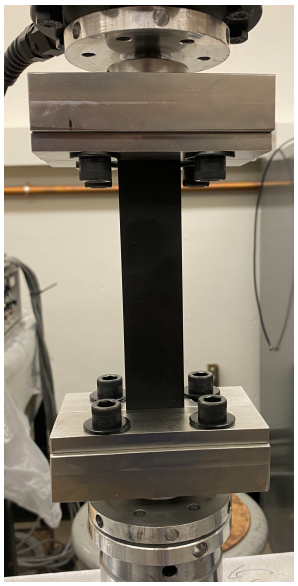

Figure 2. Uniaxial compressive buckling testing setup.

into the base, this allows accommodation for testing specimens with various thickness if desired.

For the experimental tests, first, the bases of the fixtures were attached to the top press and bottom cylinder of the testing machine. Next, the crosshead was lowered, and the sliders were put in place loosely, allowing the beam to be inserted between the top and bottom slider, and then the sliders were tightened around the beam so that the beam cannot move forwards, backwards, or to the side. This represents the fixed boundary conditions on the top and bottom edges. The compressive tests were performed with displacement control with a rate of 1 mm/min and were performed on four specimens each for both auxetic and non-auxetic specimens.

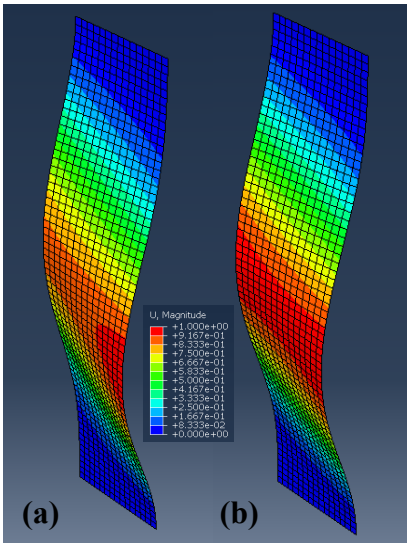

Figure 3. Predicted buckling shapes for (a) auxetic and (b) non-auxetic composites from FEA simulation.

Table II. Comparison of critical buckling loads between simulated and experimental results.

Specimen Type	Simulation (N)	Experimental (N) (average)	Percent Error (%)
Auxetic	127.33	116.37	8.61
Non-Auxetic	43.84	37.84	13.69

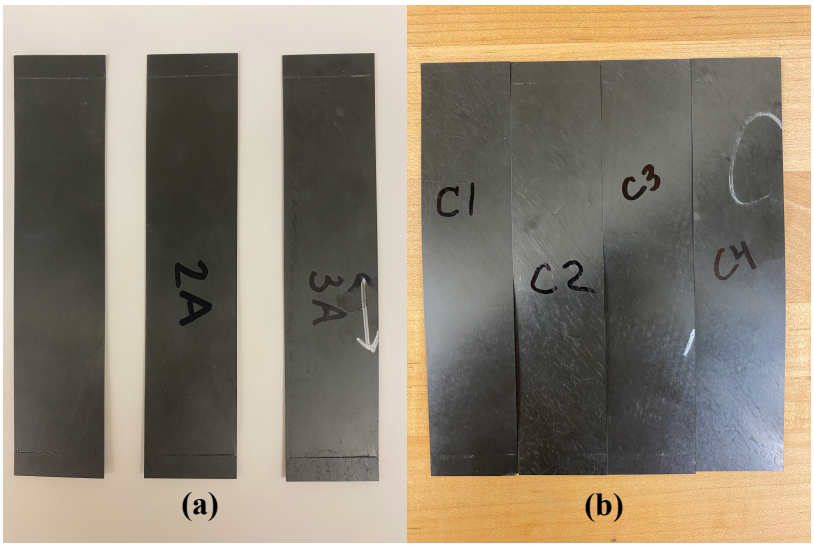

Figure 4. (a) Auxetic and (b) non-auxetic composites after uniaxial compressive buckling testing.

RESULTS AND DISCUSSION

From the FEA simulation, the predicted buckling shapes for the auxetic and non-auxetic specimens were found to be similar to each other, as shown in Figs. 3(a) and 3(b) which are the contour plots for the unified out-of-plane displacement for the auxetic and non-auxetic models, respectively. The critical buckling loads calculated are shown in Table II. The critical buckling load for the auxetic specimen was found to be 127.3 N which was approximately three times higher than the non-auxetic specimen, with a critical buckling load of 43.8 N.

From the uniaxial compressive tests, the main failure for the composite specimens after experimental tests occurred at the edges of the sliders where the composites met the fixture at both the top and bottom as shown in Figs. 4(a) and 4(b), this could be due to the extended amount of displacement applied during loading. In addition to the physical change in shape and damage, the critical buckling loads were also determined. The experimental critical buckling load for each specimen was found by finding the point of interaction for the stable loading path and the post buckling equilibrium path from the Load vs. Displacement curves generated during the tests. The critical buckling loads from the experimental tests are presented also in Table II. For the experimental tests, the average critical buckling load of the four tests for the auxetic specimens was 116.37 N while the average for the non-auxetic specimens was 37.84 N.

For the graphs of Load vs. Displacement, the FEA simulations of both the auxetic and non-auxetic have steep slopes to their respective critical buckling loads, after this point, the forces increase much slower as the vertical displacement increases, as displayed in Fig. 5. For the experimental test results for the auxetic specimens,

specimens 1 and 4 increased steeply then both increased much slower until they flattened out as the vertical displacement increased with specimen 1 stalling just above 120 N and specimen 4 stalling just above 100 N. Specimens 2 and 3 increased to much higher values, then their forces increased much slower as the vertical displacement increased until the force for specimen 2 flattened out around 120 N and the force for specimen 3 flattened out above 120 N. These results are presented in Fig. 6. For the experimental test results for the non-auxetic specimens, the forces for all 4 specimens increased steeply. As the vertical displacement increased, the forces for all specimens increased slowly and then samples 1, 2, and 4 flattened out around 35 N while sample 3 flatted out around 30 N. These results are presented in Fig. 7.

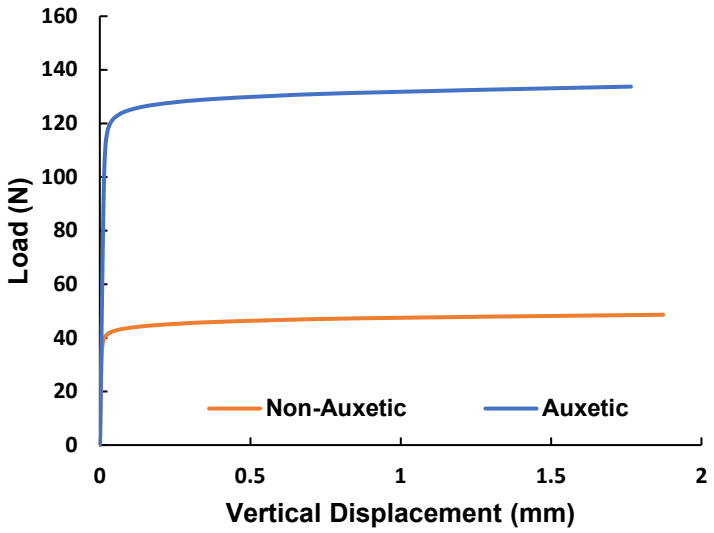

Figure 5. Simulation Load vs. Displacement results for auxetic and non-auxetic specimens.

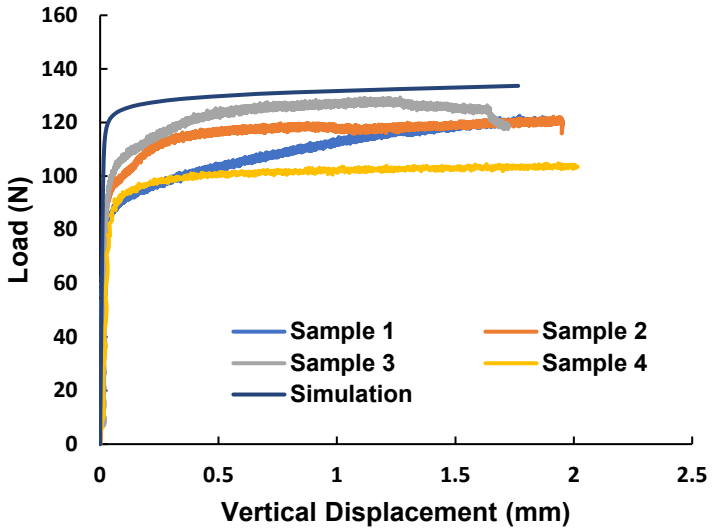

Figure 6. Load vs. Displacement curves from experimental tests for auxetic specimens.

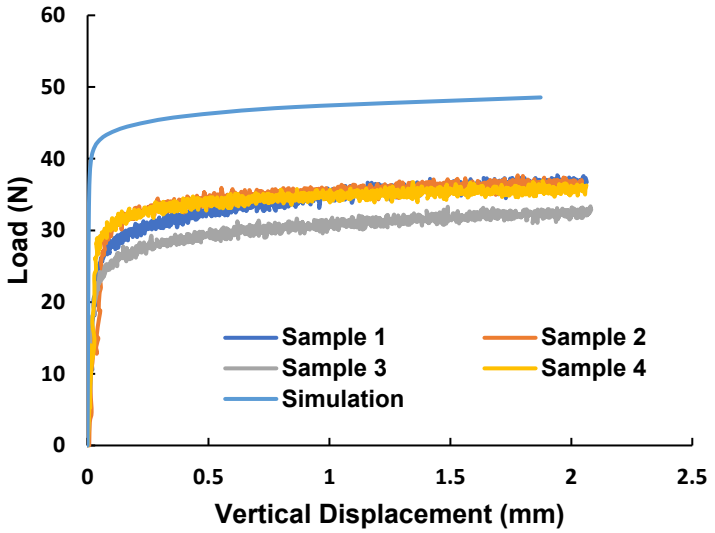

Figure 7. Load vs. Displacement curves from experimental tests for non-auxetic specimens.

CONCLUSION

During this project, the effectiveness of auxetic composites under buckling loads in comparison to non-auxetic composites was investigated. Using the obtained experimental test results, the accuracy of simulation results for composite materials was also studied. The experimental results were obtained using an MTS universal testing machine to apply compressive loads while the simulation results were performed in Abaqus. In both the experimental and simulated tests, the critical buckling loads for the auxetic composites were about 3 times higher than the critical buckling loads for the non-auxetic composites. Despite this, more research is needed to determine if other factors were contributing to the increased critical buckling loads. Specifically, for the auxetic composite, there was higher accuracy between the simulated critical buckling load and the average experimental load than for the non-auxetic composites. Along with this, the experimental results for the auxetic specimens were much more scattered than for the non-auxetic specimens. Therefore, more testing and simulation are needed to determine whether the difference between the two results lies in the simulated model, the implementation of the FEA simulations, or the experimental testing. Along with this, the inaccuracy of the nonlinear behavior in simulation compared to the nonlinear behavior in testing shows that the simulation may not be able to accurately predict how the composite will react once it enters its nonlinear region. Altogether, more testing and simulation work is required to determine the true effect of auxeticity on the critical buckling load of composite materials.

ACKNOWLEDGMENTS

The authors would like to acknowledge the financial support from National Science Foundation under Award No. CMMI-2202737.

REFERENCES

1. Dexcraft. “Carbon Fiber Composites: Properties: Manufacturing Methods: Pros and Cons.” *Carbon Fiber Blog*, 4 Dec. 2018, www.dexcraft.com/carbon-fiber-composites.
2. Bhatt, Pooja, and Alka Goe. “Carbon Fibres: Production, Properties and Potential Use.” *Material Science Research India*, vol. 14, no. 1, 2017, pp. 52–57, https://doi.org/10.13005/msri/140109.
3. “Ultimate Guide to Carbon Fiber Design & Application.” *Element6 Composites*, 2 Feb. 2023, element6composites.com/a-comprehensive-guide-to-carbon-fiber-design-and-application/.
4. Burgess, Kelly. “Carbon Fiber in Everyday Applications.” *Composites One*, 6 Apr. 2018, www.compositesone.com/carbon-fiber-in-everyday-applications/.
5. “The Many Exciting Uses of Carbon Fiber in Composites Manufacturing.” *Trade School In Newport, RI*, www.iyrs.edu/iyrs-blog/blog-details-page/~board/student-blogs/post/the-many-exciting-uses-of-carbon-fiber-composites#:~:text=Hockey%20sticks%2C%20tennis%20racquets%2C%20archery,carbon%20fiber%20helmets%20and%20shoes. Accessed 27 May 2023.
6. Burgess, Kelly. “Carbon Fiber in Everyday Applications.” *Composites One*, 6 Apr. 2018, www.compositesone.com/carbon-fiber-in-everyday-applications/.
7. Harussani, M.M., et al. “Recent Applications of Carbon-Based Composites in Defence Industry: A Review.” *Defence Technology*, vol. 18, no. 8, 2022, pp. 1281–1300, https://doi.org/10.1016/j.dt.2022.03.006.
8. Röding, Tim, et al. “A Review of Polyethylene-based Carbon Fiber Manufacturing.” *Applied Research*, vol. 1, no. 3, 2022, https://doi.org/10.1002/appl.202100013.
9. Johnson, Todd. “What Is Carbon Fiber Used For?” *ThoughtCo*, 22 June 2018, www.thoughtco.com/uses-of-carbon-fiber-820394.
10. “Composite Materials, Carbon Fiber, Uses and Applications of Carbon Fiber.” *LeapTech Composite Materials and Parts*, www.carbonfiberglass.com/composite-resources/composites-articles/Uses-Applications-Carbon-Fiber. Accessed 28 May 2023.
11. Pinto, Rochele, et al. “Mechanical Properties of Carbon Fibre Reinforced Composites Modified with Star-Shaped Butyl Methacrylate.” *Journal of Composite Materials*, vol. 56, no. 6, 2022, pp. 951–959, https://doi.org/10.1177/00219983211065206.
12. Wang, Jiayi, et al. “Research on Tensile Properties of Carbon Fiber Composite Laminates.” *Polymers*, vol. 14, no. 12, 2022, p. 2318, https://doi.org/10.3390/polym14122318.
13. De Luca, Francois, et al. “Increasing Carbon Fiber Composite Strength with a Nanostructured ‘Brick-and-Mortar’ Interphase.” *Materials Horizons*, vol. 5, no. 4, 2018, pp. 668–674, https://doi.org/10.1039/c7mh00917h.
14. Thushanthan, Kannan, et al. “Experimental Study on Tensile Strength Degradation of Carbon Fiber Reinforced Polymer (CFRP) Composite in Alkaline Environment.” *2022 Moratuwa Engineering Research Conference (MERCon)*, 2022, https://doi.org/10.1109/mercon55799.2022.9906247.
15. Sehar, Bakhtawar, et al. “The Impact of Laminations on the Mechanical Strength of Carbon-Fiber Composites for Prosthetic Foot Fabrication.” *Crystals*, vol. 12, no. 10, 2022, p. 1429, https://doi.org/10.3390/cryst12101429.
16. Singh, Priyanka, et al. “Synthesis of Carbon Fiber Composites and Different Methods to Improve Its Mechanical Properties: A Comprehensive Review.” *IOP Conference Series: Earth and Environmental Science*, vol. 889, no. 1, 2021, p. 012013, https://doi.org/10.1088/1755-1315/889/1/012013.
17. Evans, Ken E. “Auxetic Polymers: A New Range of Materials.” *Endeavour*, vol. 15, no. 4, 1991, pp. 170–174, https://doi.org/10.1016/0160-9327(91)90123-s.
18. Lin, W. & Wang, Y. (2023). Low velocity impact behavior of auxetic CFRP composite laminates with in-plane negative Poisson’s ratio. Journal of Composite Materials, 57(12):2029-2042.
19. Wang, Y. (2022). Auxetic Composite Laminates with Through-Thickness Negative Poisson’s Ratio for Mitigating Low Velocity Impact Damage: A Numerical Study. Materials, 15, 6963.

20. Fan, Y., & Wang, Y. (2021). The effect of negative Poisson's ratio on the low-velocity impact response of an auxetic nanocomposite laminate beam. International Journal of Mechanics and Materials in Design, 17(1), 153-169.
21. Fan, Y., & Wang, Y. (2020). A Study on Effect of Auxeticity on Impact Resistance of Carbon Nanotube Reinforced Composite Laminates. In Proceedings of the American Society for Composites—Thirty-fifth Technical Conference. DOI: 10.12783/asc35/34959.
22. "Design Simulation." *Siemens Digital Industries Software*, www.plm.automation.siemens.com/global/en/our-story/glossary/design-simulation/13152. Accessed 28 May 2023.
23. Lin, W., & Wang, Y. (2022, September). Effect of Negative Poisson's Ratio on the Tensile Properties of Auxetic CFRP Composites. In *Proceedings of the 37th American Society for Composites Conference and ASTM D30 Meeting, Tucson, AZ, USA* (pp. 19-21). DOI: 10.12783/asc37/36413.